



Research Article

## Experimental effect of inclination on the process of melting paraffin in a square cavity

Hocine GUELLIL<sup>1,\*</sup> , Abdel Illah Nabil KORTI<sup>1,\*</sup> 

<sup>1</sup>ETAP Laboratory, University of Tlemcen, 230, 13000, Algeria

### ARTICLE INFO

#### Article history

Received: 26 April 2020

Accepted: 5 June 2020

#### Keywords:

Thermal Storage,  
Latent Heat, PCM,  
Paraffin, Melting Front

### ABSTRACT

Phase change material PCM is a promising strategy for reducing energy consumption in various applications. Among the large number of PCMs studied in the literature, paraffin are considered to be promising for latent heat thermal energy storage LHTES due to its appropriate thermal properties and their chemical stability. The interest of this work is to carry out an experimental procedure to visualize the phase change process of paraffin in a square cavity at different inclination angles. This article reveals how the melting rate could be affected by changing three orientations 90° (vertical heating), 0° (bottom horizontal heating) and 45° (inclined heating). The enclosure is heated on one side while the other walls are thermally insulated. The numerical photos, infrared thermal image and thermocouples-temperatures recorded during the melting processing are used to calculate the melting fractions and to estimate the intensity of heat transfer in different angles. The results show that the inclination angle has a great influence on the behavior of natural convection, affecting the front melting propagation and heat transfer rate. When the inclination angle decreases from 90° to 0° the convection currents in the cavity progressively evolve from a dominant single-cell movement to an unstable Rayleigh-Benard movement. The total melting time for the bottom and inclined heating cavities were, on average, 56% and 45% less than that of the vertical heating, respectively.

**Cite this article as:** Hocine G, Abdel I N K. Experimental effect of inclination on the process of melting paraffin in a square cavity. J Ther Eng 2021;7(7):1671–1682.

### INTRODUCTION

Using PCM in the thermal industries has become a key area of research over the past three decades. During the phase change process of PCM large amounts of heat can be stored or released. Thus, PCMs can play an important role, since excess energy available during off-peak periods

can be stored in PCM devices for later use. Due to the advantages of the durability of the physical and chemical properties and the cooling phenomenon, organic PCMs were commonly chosen for the application of LHTES in a previous works. Numerical and experimental studies have

#### \*Corresponding author.

\*E-mail address: [guellil10@yahoo.fr](mailto:guellil10@yahoo.fr), [korti72@yahoo.fr](mailto:korti72@yahoo.fr)

*This paper was recommended for publication in revised form by Regional Editor Emre Alpman*



been carried out on the phase change phenomenon since the periods of Clapeyron (1831) and Stefan (1891) until today. These works try to master the heat mechanisms that develop during the fusion of PCMs in order to accelerate the heat transfer process. However, most organic PCMs have poor thermal conductivity, these delays the duration of the thermals charge and discharge. Researchers used different methods to solve this problem, including adding finned tubes of different configurations, inserting a metal matrix into the PCM, injecting nano-conductors, distributing different materials with high conductivity and microencapsulation of PCM [1].

Valan et al. [2] have studied numerically the fusion of a nano PCM (paraffin wax with alumina) in a square enclosure of dimensions (25 mm × 25 mm) heated both by bottom and by side. They found that the shape of the front of fusion depends on the thickness of the liquid layer developed during melting, the multicellular flow was developed in the liquid phase when heating by bottom, and only one cell flow is developed when heating by side. The rate of fusion decreases with increasing volumetric composition of alumina ( $Al_2O_3$ ) for both heating systems by bottom and by side. In addition, the melting rate and the stored energy are more important for heating by side than that by bottom. Korti et al. [3] studied experimentally the process of charging and discharging of the cylindrical LHTES filled by three types of paraffin. They treated the effects of HTF inlet temperature, mass flow rate and type of PCM during the two processes (charge and discharge). The inlet temperature has a significant effect on the performance of the thermal unit and can accelerate the charging phase by 54.5% and delay the discharging phase by 48.5%. Adding engine oil to paraffin can improve the velocity of the charging and discharging process by 42.4 and 66% respectively.

The thermal behavior during the melting of PCM is strongly affected by the nature of natural convection in the liquid phase, and therefore the orientation of the strength of buoyancy. Few investigators have studied the influence of the inclination angle on the PCM melting process in the enclosure. Senthil et al. [4] studied numerically using the enthalpy-porosity approach the thermal behavior of PCM in a cavity at different inclinations of 0°, 45°, 135°, 180° and 225°. They found that the melting time of the horizontal enclosure was less than half that of the vertical enclosure. Natural convection intensity was found to be lower for 45° than for the other inclinations. Indeed, the heat is transferred naturally from bottom to top. An inclination of 225° causes the shortest time for a complete fusion. Therefore, system inclination can modify the melting velocity. Natural convection in liquid PCM is highly dependent on the location of the warm wall. The liquid fraction for a horizontal orientation is greater than that of the vertical orientation. Madruga et al. [5] simulated the fusion dynamics of the n-octadecane PCM on two square geometries with 1 and 2 cm sides and subjected to lateral

heating. They calculated the overall rate of the liquid fraction when convective movements are caused only by buoyancy and when thermo-capillary flows are included. The flow and temperature field functions made it possible to follow the dynamic evolutions of the fusion. They found that the overall evolution of the solid / liquid interface is similar for the two geometries. The same thing happens when the thermocapillary line is superimposed. The last case produces a very rapid detachment of the solid / liquid front from the upper free surface. From the results, they concluded that the thermo-capillary effects have a very relevant mechanism for improving the rate of heat transfer to n-octadecane, especially when it is subjected to high outside temperatures. In second study, [6] have studied numerically the dynamic behavior during the fusion of n-octadecane in a cavity heated from bottom through varying lengths ranging from 0.005 to 0.2 m. They have identified four different regimes over time: (i) conductive regime, (ii) linear regime, (iii) coarsening regime and (iv) turbulent regime. They found that conduction generates a front whose shape is dictated by geometry. The second regime leads to linear Rayleigh Benard instability which creates a network of symmetrical convective cells with opposite rotation whose peaks correspond to the position of the plumes in the form of mushrooms. The coarsening regime induces the enlargement and the shape of the head which are responsible for creating a solid/curved liquid interface. Finally, the turbulent regime leads to a very irregular solid/liquid interface with large fluctuations in the amplitude. They also concluded that the separation between the plumes is determined by the critical wave number of the Rayleigh-Benard primary instability. Consequently, this wave number determines the distance between the peaks of the melting front. In a third study, [7] performed a comparative analysis of experimental results and numerical simulations of fusion of the tetracosane PCM contained in a cube and heated from bottom, while all the other sides are assumed to be adiabatic. They observed the behavior of the solid/liquid interface throughout the experiment, characterized by an irregular shape. They visualized the behavior of the isotherms, as well as the speed field corresponding to the turbulent regime. Thus the observation of the solid/liquid interface is a useful measure to identify the overall melting state and internal thermal (plumes) and velocity (convective cells) regime. Among the experimental investigators, Kamkari et al [8] studied the dynamic thermal behavior of PCM (Lauric acid with range of melting 43.5–48.2°C) melting in a rectangular enclosure at various inclination angles (vertical, bottom and 45° inclination). The enclosure is heated isothermally from one side while the other walls are thermally insulated. For the same hot wall temperatures, the total melting time for the inclined and bottom cases were, on average, 35% and 53% less than the vertical case, respectively. The time-averaged Nusselt number showed

11% and 35% enhancements when the wall temperature was increased from 55 to 60 and 70°C, respectively. Guellil et al. [9] studied experimentally the performance of a novel LHTES unit using a finned U-tubes exchanger filled with paraffin. The study observed that using the fins improves the energy stored more than five times. Increasing the power supply by 32% decreases the average melting interval by 34% and delays the time of solidification starting by about 30%. Huang et al [10] developed a PV/PCM digital model and validated it experimentally. The digital model uses a PCM (RT25) to moderate the temperature rise of the PV which is validated for geometries of identical size with realistic experimental conditions. The validated model provided a detailed overview of the thermal performance of the solid-liquid transition PCM when used in a PV temperature control application. The improvement in thermal performance is obtained by using metal fins in the PCM container. These fins helped maintain a more uniform temperature distribution in the PV/PCM system.

After the selection of the PCM type, the geometry of the PCM container is the most influential factor in the thermal performance of PCM systems. Some studies have been concerned with the heat transfer in square cavities heated from the side. The melting of RT44HC has been explored experimentally in a rectangular cavity heated from both the left and right sides [11]. The result showed a strong correlation between the amplitude of the heat flow from the wall and the melting fraction in the PCM due to

heat transfer by convection. F. Mehdaoui et al [12] studied experimentally heat transfer phenomena in a vertical enclosure containing PCM-27 integrated inside a test cell of dimension (0.5, 0.5, 0.5 m<sup>3</sup>). They found that during the heating phase, the temperature inside the test cell equipped with the PCM-27 vertical enclosure is about 28°C. They also found that once the PCM-27 vertical enclosure was omitted, the cell temperature inside the test cell was between 29 and 40°C. The TRNSYS simulation is carried out to evaluate the feasibility of integrating the PCM-27 vertical enclosure into a real building envelop. The results of the TRNSYS simulation showed that the integration of a well-dimensioned vertical PCM enclosure improves the thermal comfort of the occupant by reducing thermal fluctuations and improving the thermal inertia of the walls. R. Zarrit et al [13] studied numerically the unsteady and two-dimensional natural convection in an inclined rectangular cavity heated differentially. The Rayleigh number was varied between ( $10^3 \leq Ra \leq 10^4$ ), the aspect ratio ( $1 \leq A \leq 6$ ) and the angle of inclination  $\theta$  between ( $0^\circ \leq \theta \leq 180^\circ$ ). They highlighted the influence of the angle of inclination and the aspect ratio on the structure of the flow and heat transfer. The results revealed the existence of a critical angle  $\theta_{cr}$  (for which an abrupt change in the value of the Nusselt number is detected) depending on the aspect ratio  $A$  and the number of Rayleigh  $Ra$ . They found that for  $\theta \approx 0^\circ$ , the flow is multicellular, which results in a remarkable increase in the number of Nusselt. For  $\theta > \theta_{cr}$ , the flow is

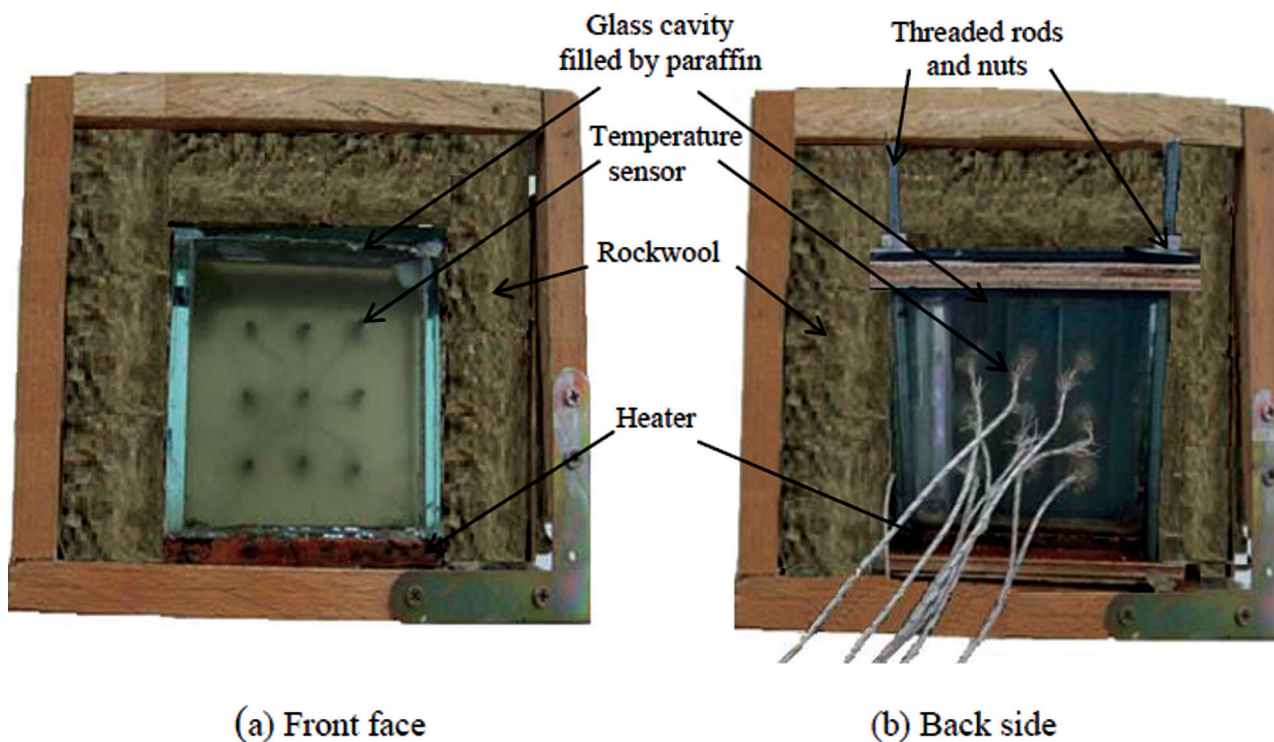


Figure 1. Picture of the cavity insulated by rockwool.



Figure 1.b. Picture of the laboratory setup.

single-cell and in the case where  $\theta \approx 180^\circ$ , the fluid stagnates and a thermal stratification is quite clear. To see the thermal contribution of a porous medium, [14] presents a numerical analysis for double-pass solar air collector with and without a porous media. The study examines the effects of porosity (70–90%), the mass flow (0.03–0.07 kg/s), the solar intensity (514–714 W/m<sup>2</sup>) and spacing glass-absorber-insulation (7–10 cm) on the dynamic and thermal behavior of double-pass solar collectors. He concludes that the presence of the porous media at the bottom of the absorber is the best configuration and allow increasing the outlet temperature.

This study presents an experimental work of a thermal cavity made by glass in order to understand and visualize the thermal behavior of a PCM (paraffin) during melting. The analysis relates to the thermal study of the effect of the inclination angle of the cavity on the phase change process. Since the majority of the work carried out in this area is

Table 1. Thermal physical properties of PCM used

Denomination	Tetracosane C <sub>24</sub> H <sub>50</sub>
Solid density at 25°C (kg/m <sup>3</sup> )	912
Liquid density at 80°C (kg/m <sup>3</sup> )	769
Melting enthalpy (kJ/kg)	162.42
Heat conductivity (W/mK)	0.2
Specific heat capacity (kJ/kgK)	2
Melting temperature range (°C)	49÷54

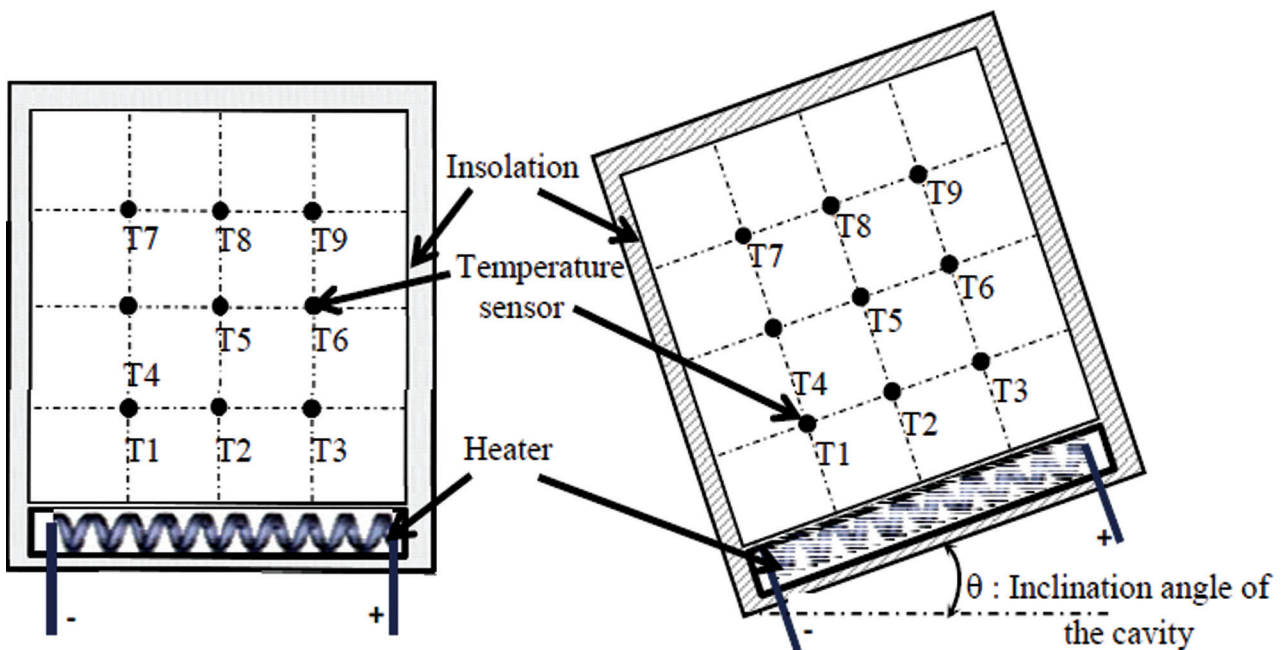


Figure 2. Schematic diagram of the experimental procedure.

based on the numerical simulation, the obtained results can be used as a benchmark model for the future work.

## EXPERIMENTAL PROCEDURE

Initially, liquid paraffin (PCM) is poured into a square thermal cavity of dimensions (12 cm × 12 cm and thickness 4.5 cm) made of glass (thickness 10 mm) to allow the visualization of PCM behavior during melting (Figure 1.a). The visualization is carried out on the front face by using a simple numerical camera and infrared camera (Testo i875) (Figure 1.b). Only one side of the cavity is heated by an electric heater which produces a constant heat flux (1.8 W) (Figure 2). This Heater is placed inside a copper cavity glued to the glass cavity. All the system is insulated using rock wool and placed in a wooden cavity. To reduce the constraints in the liquid phase during melting [14], the back face of the cavity is pierced and nine type-K thermocouples are placed on middle plan of the cavity (figure 2). The thermocouples are distributed uniformly (space 3 cm) to measure the thermal evolution of the paraffin during fusion. An NI data logger (c-DAQ 9174) is used to record the measurements. In order to see the effect of the inclination of the cavity on the thermal behavior of the paraffin melting front, three configurations are adopted: vertical heating on the right ( $\theta = 90^\circ$ ), horizontal heating on the bottom ( $\theta = 0^\circ$ ) and inclined heating ( $\theta = 45^\circ$ ), (figure 2). The upper mobile face is fixed using by four bolts to allow filling and leveling the paraffin before each experience. The thermo-physical properties of the PCM (Tetracosane) used are presented in table 1.

## RESULTS AND DISCUSSION

### Pattern of the Solid-Liquid Interface

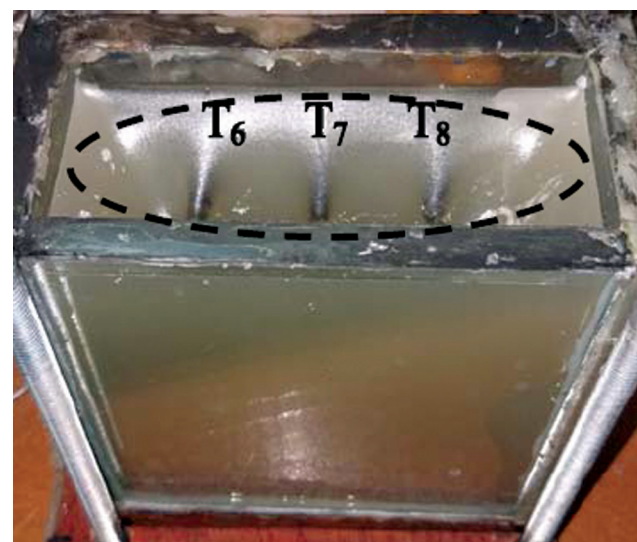
During the solid-liquid phase change of the PCM, the visualization of the melting process reveals important flow patterns and dominant heat transfer mechanisms. Figure 4 and figure 5 show the sequential photos and front melting profile during the paraffin melting process on different inclination angles the cavity ( $90^\circ$ ,  $0^\circ$  and  $45^\circ$ ). The times selected correspond approximately to the same liquid fraction evolution for different inclinations. Tetracosane (PCM) in solid phase has a white color which turns to the transparent liquid during fusion. Thus, the solid and liquid phases are represented respectively by the white and brown colors areas.

Figure 4.a and figure 5.a show the photos of melting process and melting front profiles during the vertical heating of the enclosure ( $\theta = 90^\circ$ ). During the first moments of the fusion ( $t < 10$  min), a thin layer of molten PCM appears parallel to the hot wall, indicating that the mode of heat transfer is dominated by conduction. This mode of heat transfer shows that the viscous force opposes the movement of the fluid during which the solid-liquid interface

remains almost uniform and parallel to the hot wall. As time advances, the melting front progresses and the buoyancy force becomes more important to overcome the viscous force. Natural convection current is initiated in the melting region which widens in the top layer of liquid phase (20 min). The development of the buoyancy force leads to the formation of an increasing mono-cellular current in the molten paraffin that provides the heat to rise through the hot wall and accelerates the melting at the top, and subsequently causes the descent of liquid through the melting front and delays the melting at the bottom (50 and 80 min). This melting behavior continues until the solid PCM melts completely.

We also note between 20 to 80 min, a part of the solid paraffin remains stuck on the left-top part in the form of a cap. This phenomenon is due to the shrinkage of the material during the solidification of the paraffin that creates a concave surface at the top of the paraffin after each experience (figure 3). This concave surface creates a pocket-air that disrupts the cellular movement of convection at the top of molten paraffin. This phenomenon is neglected in the vast majority of the numerical simulation works.

Figure 4.b and figure 5.b show the photos of melting process and melting front profiles during the bottom heating of the enclosure ( $\theta = 0^\circ$ ). At the start of the melting process, the solid-liquid interface is almost flat and parallel to the hot wall; the heat transfer is dominated by thermal conduction. At 30 min, the shape of the interface presents instabilities and becomes wavy. This wavy shape of the interface indicates the development of the Rayleigh Benard multicellular natural convection in liquid PCM [8]. Indeed, natural convection develops between two parallel horizontal walls, heated from bottom, in the form of



**Figure 3.** Pocket-air due to the shrinkage of the PCM after solidification.

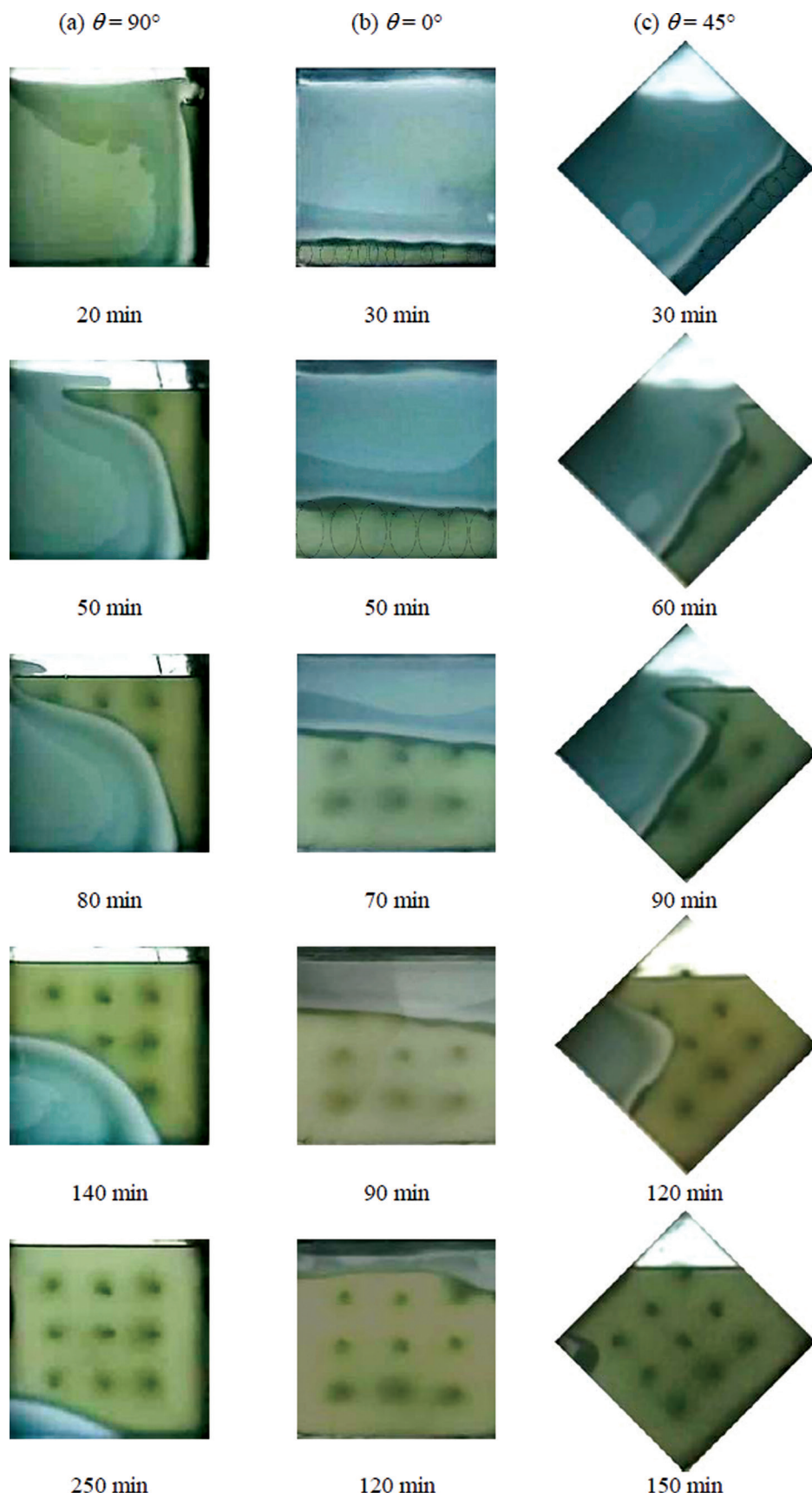


**Figure 4.** Time evolution of the melting process of the heated paraffin for 3 different angles.

Rayleigh Benard counter-rotating rollers. The number and shape of these rollers depend on the temperature gradient and the size of the cavity. According to the literature [15], around eleven counter-rotating rollers are observed in the liquid phase. As the fusion progresses (50 to 90 min), the convection cells merge with the neighboring cells and become larger leading to a decrease in the number of cells [13]. At the end of the fusion process (90 to 120 min), the convection cells join and a single dominant cell is observed. The total paraffin fusion is achieved after 140 min (3 hours before the case of vertical heating  $90^\circ$ ) with a volumetric expansion of the order of 3%.

Figure 4.c and figure 5.c show the photos of melting process and melting front profiles during the inclined

heating of the enclosure ( $\theta = 45^\circ$ ). Unlike Figure. 4.a, a thin layer of molten paraffin appears at the bottom of the enclosure and at a vicinity of the hot wall, after 30 min. However, the melting interface presents Rayleigh-Benard instabilities due to the phenomenon of natural convection which develops earlier in the form of six counter-rotating rollers. Thus, the inclination of the cavity caused the decrease of the cellule number six rollers (50%) compared to the bottom heating cavity. Indeed, the literature [8,13] reveals that the number of counter-rotating rollers developed in a cavity heated from below decreases with increasing the inclination angle of cavity. At 60 min, we observe the beginning of formation of the cap phenomenon (due to the shrinkage of the material due to solidification) which develops and becomes more visible after 90 min at the top surface of the paraffin. The melting curvature indicates that the liquid PCM is heated by the hot wall, and flows parallel to the hot wall as in the vertical case. It goes up to the top surface of paraffin and develops the cap phenomenon. This accelerates the melting speed at the top of the liquid phase and indicates the presence of the first cellule. After 120 min, the acceleration of the melting speed at the bottom corner indicates the presence of the second cellule. The last still solid part of the paraffin remains stuck in the left corner of the cavity and the fusion reaches 73.8%. The paraffin melting ends after 165 min. It represents 155 min before the vertical heating case  $90^\circ$  and 25 min after the bottom heating case.

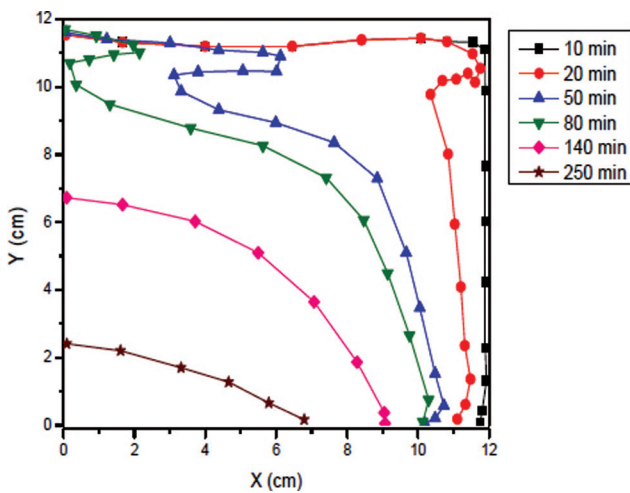


Figure 5.a. Time evolution of the position and shape of the melting front for vertical heating ( $\theta = 90^\circ$ ).

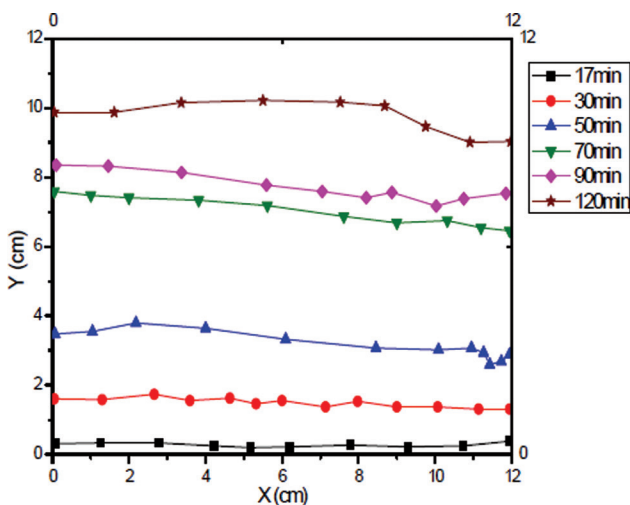


Figure 5.b. Time evolution of the position and shape of the melting front for bottom heating ( $\theta = 0^\circ$ ).

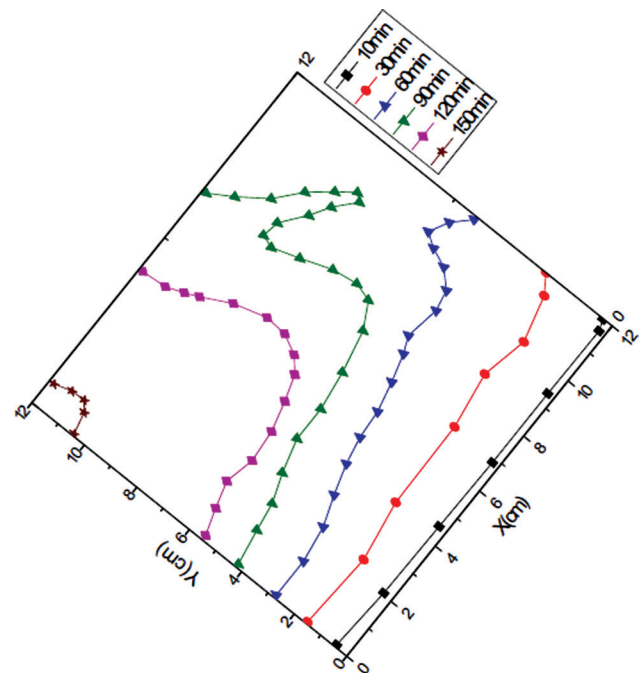


Figure 5.c. Time evolution of the position and shape of the melting front for inclined heating ( $\theta = 45^\circ$ ).

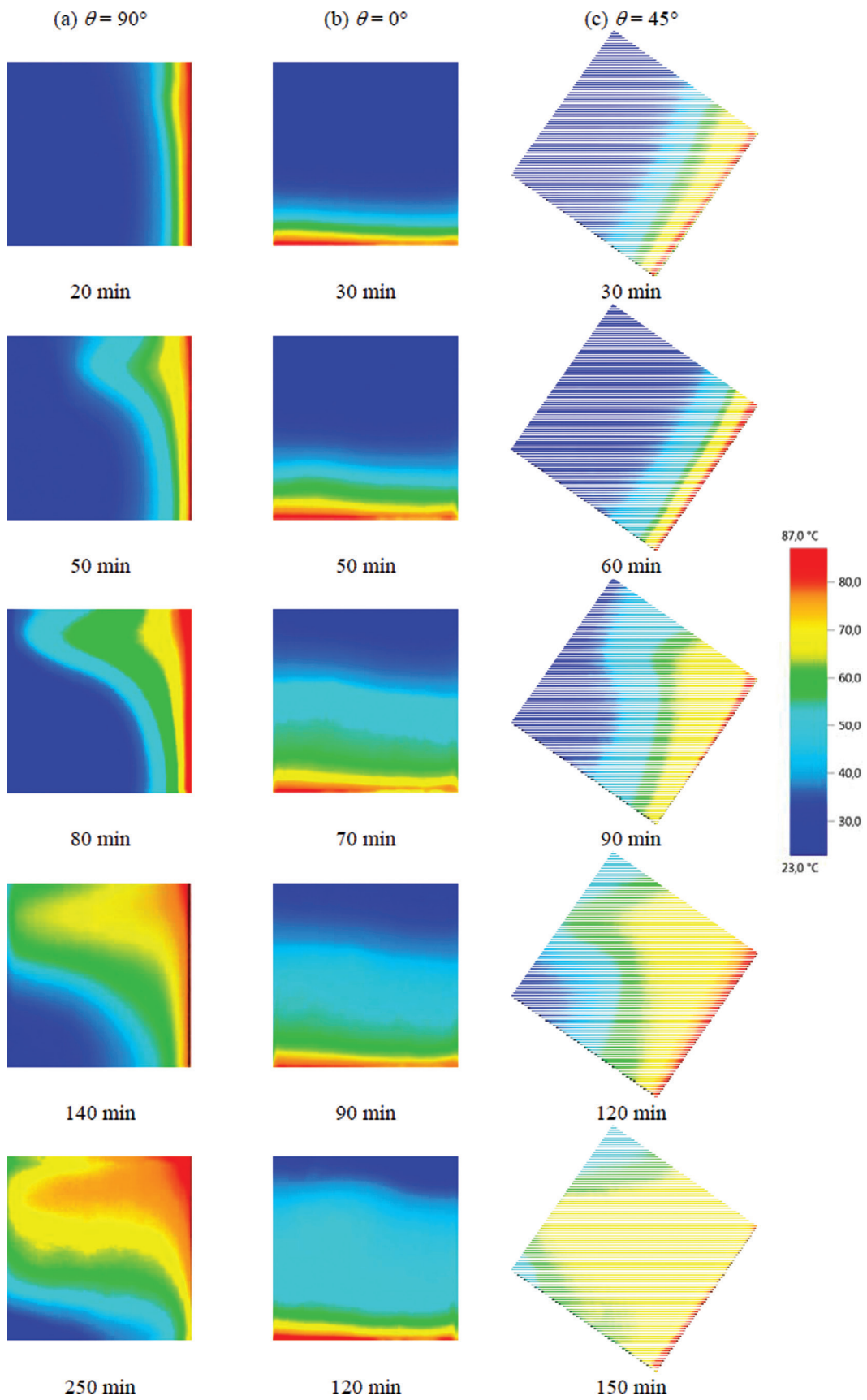


Figure 6. Infrared image of the temperature field for 3 different angles.

### Temperature Distribution

To the better understand the behavior of convection heat flow during the melting of paraffin; an infrared camera was used to record the temperature field in the front face of cavity for the three different angles (Figure 5). In addition, Figure 6 represents the time evolution of the position and the shape of the solid-liquid interface estimated from Figure 3 according to the 3 inclinations.

Figure 6.a shows the time evolution of the temperature field profile in the vertical heating ( $\theta = 90^\circ$ ). Overall, the solid is identified by the blue color and the liquid phase by the other colors. During the first moments of melting, the heating starts in the vicinity of the heat source and the temperature profiles are in the form of straight lines parallel to the hot wall whose the temperature range is between 50–70°C. This justifies that the heat transfer is dominated by conduction at this stage of melting process (until 20 min). Later between 50 and 80 min, the temperature of the liquid PCM adjacent to the hot wall increases enough and the buoyancy force overcomes the viscous force leading to the rising of the hot liquid PCM along the vertical hot wall. When the hot liquid PCM reaches the top of the cavity, it flows toward the left and goes down through the melting front. Thus, we can see the curvature of the isotherms at the top of the cavity indicating the anticlockwise cell that develops in the liquid phase. This cell accelerates the heat transfer at the top of the cavity and slows down the heat transfer at the bottom. The mushy zone that represents the temperature range of melting is observed between 48–54°C. After 140 min, the speed of the melting rate decreases due to its distance from the heat source. As a result, the intensity of natural convection developed in the liquid phase decreases and the solid-liquid exchange surface decrease over time. At 250 min, a small quantity of paraffin solid exist in the lower left part of the cavity (dominated by conduction) whose temperature is in the range of 30 ÷ 40°C. On the other hand, the temperature gradient in the liquid part is higher and varies between 54–80°C.

Figure 6.b shows the time evolution of the temperature field profile in the bottom heating ( $\theta = 0^\circ$ ). It is observed that the temperature gradient in the liquid phase is clearly greater than in the solid phase. Therefore, the convection movement accelerates the heat transfer in the liquid phase. Due to the poor thermal conductivity of the paraffin, the heat transfer by conduction in the solid phase is low. The isotherms evolve over time in an almost stratified way due to the large number of Rayleigh-Benard convection cells developed in the liquid phase, which are responsible for the good heat transfer from the hot wall to the solid existing always at the top of the cavity.

Figure 6.c shows the time evolution of the temperature field profile in the inclined heating ( $\theta = 45^\circ$ ). Compared to the vertical heating, the isotherms remain stratified until 60 min. Initially, the heat transfer is dominated by conduction and develops after to a Rayleigh-Benard multi-cellular

convection. At 90 min, the isotherms become curved at the top of the paraffin and the heat is dominated by single-cell convection in the liquid phase. After 120 min, heat transfer is accelerated in the lower corner showing a development of a single cell in this region.

### Temperature History

Figure 7 shows the temperature profiles of the PCM in the cavity at different inclination angles. Overall, the recorded temperatures at different locations increase initially due to thermal conduction in the solid PCM until the melting temperature is reached. During this duration, the local temperature near the heating wall increases more quickly than that the other locations. This can be explained by the low thermal conductivity of paraffin and the fact that the heat transfer in the solid PCM takes place by a thermal conduction through the thin layer of the liquid PCM.

Figure 7.a shows the time evolution of the temperature during the melting of the paraffin for the vertical heating ( $\theta = 90^\circ$ ). In practice, it is so difficult to impose a constant temperature on the heating wall. Thus, imposing a constant flow leads to a progressive increase of the temperature of heating wall  $T_0$  that stabilizes around 98°C (4°C), after 45 min. At the beginning, the temperatures  $T_8$ ,  $T_7$  and  $T_6$  (top region of paraffin) increase rapidly to reach respectively a maximum of 78, 74 and 75°C around 44, 75 and 91 min. After 92 min, these temperatures become almost identical and start to stabilize reaching around 85°C at the end. Because of the natural convection developed within the liquid phase, the first melting location is around  $T_8$  at 40 min and the last region around  $T_0$  at 224 min. The start of the melting location does not depend only on its distance from the hot wall. Indeed, by approaching the hot wall and going upwards, the melting starts quickly. This indicates the presence of the single-cell convection flow in the liquid phase. At 250 min, the temperatures at the upper, middle and lower level become identical and reach respectively 82, 77 and 70°C to stabilize around 85, 81 and 75°C at the end. Thus, horizontal stratification of temperatures is observed indicating convection heat flow domination.

Figure 7.b shows the time evolution of the temperature during the melting of the paraffin for the bottom heating ( $\theta = 0^\circ$ ). The temperature of heating wall  $T_0$  increase progressive and stabilizes around 90°C ( $\pm 1^\circ\text{C}$ ), after 55 min. The hot wall temperature stabilizes at a temperature lower than the vertical case by 8°C. Thus, the heat energy extracted by the paraffin is more important in the bottom heating case and accelerates the melting process. At the start, the paraffin begins to melt from the bottom due to the phenomenon of conduction. After 17 min, the temperatures at the lower level near to the hot wall ( $T_0$ ,  $T_1$ , and  $T_2$ ) increase together and more quickly to stabilize with fluctuations around 70°C after 65 min. These fluctuations are due to the Rayleigh-Benard counter-rotating rollers. The temperatures at the middle level ( $T_3$ ,  $T_4$ , and  $T_5$ ) and top level ( $T_6$ ,  $T_7$ , and  $T_8$ )

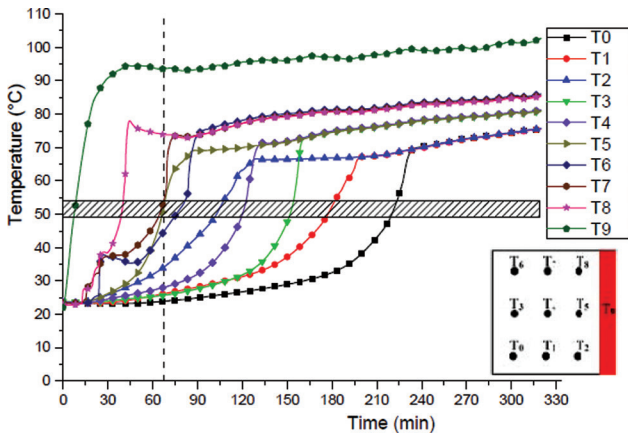


Figure 7.a. Temporal evolution of paraffin temperature for the vertical cavity.

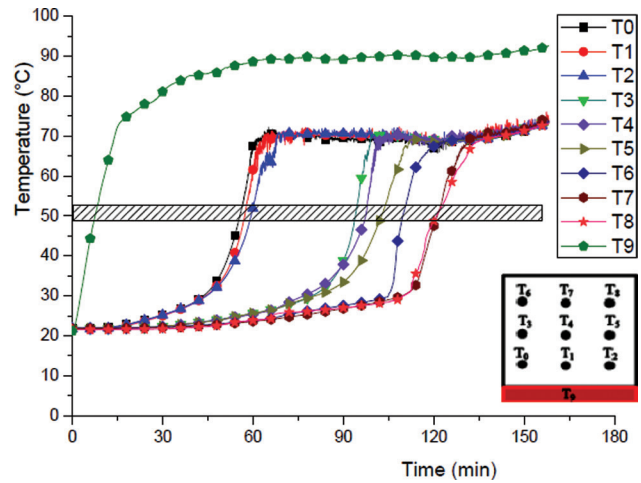


Figure 7.b. Temporal evolution of paraffin temperature for the horizontal cavity.

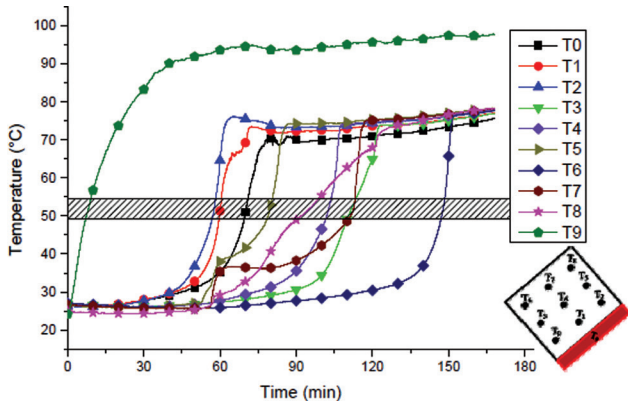


Figure 7.c. Temporal evolution of paraffin temperature in a 45° inclined cavity.

increase also together in the temperature range to stabilize around the same temperature 70°C after 65 min. The temperature range indicates the merging and the decrease in the number of the Rayleigh-Benard counter-rotating rollers. At the end, no temperature stratification is observed and the paraffin reaches a uniform temperature around 70°C after 125 min.

Figure 7.c shows the time evolution of the temperature during the melting of the paraffin for the inclined heating ( $\theta = 45^\circ$ ). The temperature of heating wall  $T_9$  increase progressive and stabilizes around 96°C ( $\pm 2^\circ\text{C}$ ), after 60 min. The hot wall temperature stabilizes at a temperature higher than the bottom case by 6°C. Thus, the heat energy extracted by the paraffin is more important in the bottom heating than the inclined case and after than the vertical case. The temperature evolution shows that the physical phenomena influencing the heat transfer is the result of the combination of the two previous cases (heating from below and heating from the side). At the start, the temperatures  $T_2$ ,  $T_1$ , and  $T_0$

rise rapidly until reaching 76, 73 and 70°C after 66, 72 and 77 min, respectively. This evolution in temperature shows that natural convection is already present in the liquid phase. The quick increasing of  $T_5$  and  $T_7$  indicate the development of natural convection leading to the acceleration of heat transfer along the hot wall and the right face of cavity. This phenomenon confirms the development of a single-cell movement [16,17,18] in the liquid phase. The thermal equilibrium is reached around 150 min and the paraffin reaches a uniform temperature around 77°C.

**Melting Rate**

Figure 8 shows the comparison between the time evolutions of the liquid fraction of paraffin for different inclination angles. The results show that the melting process passes through two different steps. At the beginning when conduction dominates heat transfer, a shorter difference is observed between the melting rates for different inclinations. After, the effect of convection increases and the melting velocity changes. The inclination angle of the cavity can, depending on the case, accelerate or delay the melting velocity. Therefore, it is possible to choose the inclination of the cavity to optimize the melting rate and process. We also note that the melting velocity increases by increasing the angle of cavity. Heating a cavity from bottom reduce the time of complete melting by (25 and 180 min) and accelerates the melting speed by (15 and 56%) compared to respectively inclined and vertical heating cavity. The time evolution of liquid fraction can be correlated by the following correlation for different angle inclinations

$$(f_l)_{bottom} = -3 \times 10^{-12} t^3 + 3.69 \times 10^{-8} t^2 + 2.042 \times 10^{-5} t - 0.0059 \tag{1}$$

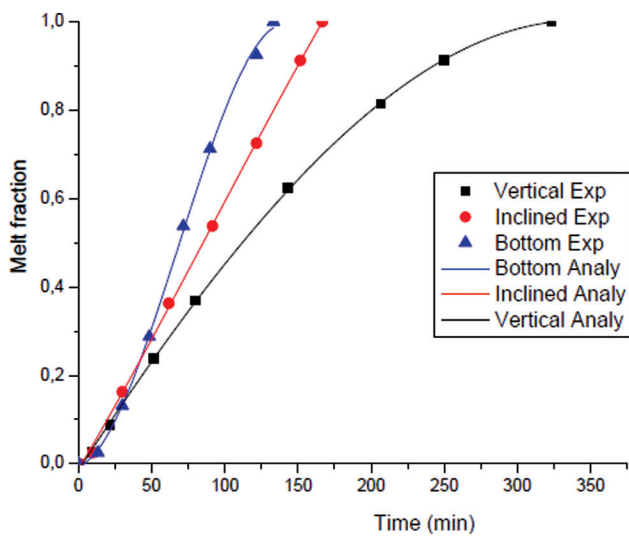


Figure 8. Time evolution of the volume fraction of liquid.

$$(f_l)_{inclined} = -1.18 \times 10^{-13} t^3 + 1.97 \times 10^{-9} t^2 + 9.34 \times 10^{-5} t - 0.013 \quad (2)$$

$$(f_l)_{vertical} = -3.39 \times 10^{-14} t^3 - 1.034 \times 10^{-9} t^2 + 8.51 \times 10^{-5} t - 0.014 \quad (3)$$

## CONCLUSION

In the present study, an experimental procedure is elaborated to analyze the effect of angle inclination on the natural convection during melting process. The PCM is placed in a square enclosure made by glass heated by one side. Paraffin was used as PCM and three angles were examined 0, 45 and 90°. The results allow drawing the following conclusions:

Two modes of heat transfer dominate the melting process, namely conduction and natural convection. Conduction governs melting at the start of the process and controls the development of fusion in the PCM. Advancing in time, the volume of liquid increases and the fusion is progressively dominated by natural convection.

A cavity heated from bottom accelerates the total melting time by about 25 min and 3 hours compared to the cavity inclined at 45° and the cavity heated vertically.

A single vortex dominates natural convection in the cavity heated vertically. The Rayleigh-Benard instabilities dominate natural convection in the cavity heated by bottom. For an inclined case, the developed Rayleigh-Benard instabilities turn into a two-cell natural convection.

In the range of temperatures considered, the total melting time for the bottom and inclined heating was reduced by an average of 45 and 56 % than the vertical heating cavity.

During solidification, a concave shape (shrinkage phenomenon of material) appears at the top PCM. This phenomenon leads the development of the cap form observed during the melting in the both cases vertical and inclined heating.

## NOMENCLATURE

$f$  Liquid fraction  
 $t$  Time, s  
 $T$  Temperature, °C

Greek symbols

$\theta$  Angle of inclination, degree

## AUTHORSHIP CONTRIBUTIONS

Authors equally contributed to this work.

## DATA AVAILABILITY STATEMENT

The authors confirm that the data that supports the findings of this study are available within the article. Raw data that support the finding of this study are available from the corresponding author, upon reasonable request.

## CONFLICT OF INTEREST

The author declared no potential conflicts of interest with respect to the research, authorship, and/or publication of this article.

## ETHICS

There are no ethical issues with the publication of this manuscript.

## REFERENCES

- [1] Dutil Y, Rousse DR, Ben Salah N, Lassue S, Zalewski L. A review on phase-change materials: Mathematical modeling and simulations, *Renew Sust Energy Rev* 2011;15:112–130. [CrossRef]
- [2] Valan AA, Arun SM. Numerical study on melting of paraffin wax with Al2O3 in a square enclosure. *Int Commun Heat Mass Transf* 2012;39:8–16. [CrossRef]
- [3] Korti AN, Tlemsani FZ. Experimental investigation of latent heat storage in a coil in PCM. *J Energy Storage* 2016;5:177–186. [CrossRef]
- [4] Senthil R, Cheralathan M. Natural heat transfer enhancement methods in phase change material based thermal energy storage. *Int J Chem Tech Res* 2017;9:563–570.

- [5] Madruga S, Mendoza C. Enhancement of heat transfer rate on phase change materials with thermocapillary flows. *Eur Phys J Spec Top* 2017;226:1169–1176. [\[CrossRef\]](#)
- [6] Madruga S, Curbelo B. Dynamic of plumes and scaling during the melting of a Phase Change Material heated from below. *Int J Heat Mass Transf* 2018;126:206–220. [\[CrossRef\]](#)
- [7] Madruga S, Haruki N. Experimental and numerical study of melting of the phase change material tetracosane. *Int Commun Heat Mass Transf* 2018;98:163–170. [\[CrossRef\]](#)
- [8] Babak K, Hossein S, Frank B. Experimental investigation of the effect of inclination angle on convection-driven melting of phase change material in a rectangular enclosure. *Int J Heat Mass Trans* 2014;72:186–200. [\[CrossRef\]](#)
- [9] Guellil H, Korti AN, Abboudi S. Experimental study of the performance of a novel latent heat charging unit on charging and discharging processes. *Heat and Mass Transf* 2019;55:855–866. [\[CrossRef\]](#)
- [10] Huang MJ, Eames PC, Norton B. Thermal regulation of building-integrated photovoltaic using phase change materials. *Int J Heat Mass Transf* 200;47:2715–2733. [\[CrossRef\]](#)
- [11] Fadl M, Philip CE. A comparative study of the effect of varying wall heat flux on melting characteristics of phase change material RT44HC in rectangular test cells. *Int J Heat Mass Transf* 2019;141:731–747. [\[CrossRef\]](#)
- [12] Mehdaoui F, Hazami M, Taghouti H, Noro M, Lazzarin R, Guizani A. An experimental and a numerical analysis of the dynamic behavior of PCM-27 included inside a vertical enclosure: Application in space heating purposes. *Int J Therm Sci* 2018;133:252–265. [\[CrossRef\]](#)
- [13] Zarrit R, Boumaza MS, Kherrou S, Dadda B. Convection naturelle dans une cavité rectangulaire inclinée de différents rapports de forme. *Revue des Energies Renouvelables* 2016;19:97–109. [\[CrossRef\]](#)
- [14] Korti AN. Numerical 3-D heat flow simulations on double-pass solar collector with and without porous media. *J Therm Eng* 2015;1:10–23. [\[CrossRef\]](#)
- [15] Khot SA, Sane, NK, Gawali, B. S. Experimental investigation of phase change phenomena of paraffin wax inside a capsule. *Int J Eng Trends Technol* 2011;2:2231–5381.
- [16] Gau C, Viskanta R, Ho CJ. Flow visualization during solid–liquid phase change heat transfer II. Melting in a rectangular cavity. *Int J Heat Mass Trans* 1983;10:183–190. [\[CrossRef\]](#)
- [17] Korti AN. Numerical simulation on the effect of latent heat thermal energy storage unit. *J Therm Eng* 2016;2:598–606. [\[CrossRef\]](#)
- [18] Sharifi N, Robak CW, Bergman TL, Faghri A. Three-dimensional PCM melting in a vertical cylindrical enclosure including the effects of tilting. *Int J Heat Mass Transf* 2013;65:798–806. [\[CrossRef\]](#)